

8-15-2022 10:00 AM

Intracardiac Ultrasound Guided Systems for Transcatheter Cardiac Interventions

Hareem Nisar, *The University of Western Ontario*

Supervisor: Peters, Terry M., *Robarts Research Institute*

A thesis submitted in partial fulfillment of the requirements for the Doctor of Philosophy degree in Biomedical Engineering

© Hareem Nisar 2022

Follow this and additional works at: <https://ir.lib.uwo.ca/etd>



Part of the [Biomedical Engineering and Bioengineering Commons](#)

Recommended Citation

Nisar, Hareem, "Intracardiac Ultrasound Guided Systems for Transcatheter Cardiac Interventions" (2022). *Electronic Thesis and Dissertation Repository*. 8737.
<https://ir.lib.uwo.ca/etd/8737>

This Dissertation/Thesis is brought to you for free and open access by Scholarship@Western. It has been accepted for inclusion in Electronic Thesis and Dissertation Repository by an authorized administrator of Scholarship@Western. For more information, please contact wlsadmin@uwo.ca.

Abstract

Transcatheter cardiac interventions are characterized by their percutaneous nature, increased patient safety, and low hospitalization times. Transcatheter procedures involve two major stages: navigation towards the target site and the positioning of tools to deliver the therapy, during which the interventionalists face the challenge of visualizing the anatomy and the relative position of the tools such as a guidewire. Fluoroscopic and transesophageal ultrasound (TEE) imaging are the most used techniques in cardiac procedures; however, they possess the disadvantage of radiation exposure and suboptimal imaging. This work explores the potential of intracardiac ultrasound (ICE) within an image guidance system (IGS) to facilitate the two stages of cardiac interventions.

First, a novel 2.5D side-firing, conical Foresight ICE probe (Conavi Medical Inc., Toronto) is characterized, calibrated, and tracked using an electromagnetic sensor. A point-to-line registration technique is employed to perform the calibration, which is validated using two geometric phantoms. The results indicate an acceptable tracking accuracy within some limitations. A texture mapping-based 3D Slicer module is also developed to visualize the unique conical geometry of the Foresight ICE probe.

Next, an IGS is developed for navigating the vessels without fluoroscopy. A forward-looking, tracked ICE probe is used to reconstruct the vessel on a phantom which mimics the ultrasound imaging of an animal vena cava. Deep learning methods are employed to segment the complex vessel geometry from ICE imaging for the first time. The ICE-reconstructed vessel was compared to the CT-segmented version of the vessel, which showed a clinically acceptable range of accuracy. The average surface distance error was recorded to be less than a millimeter.

Finally, a guidance system was developed to facilitate the positioning of guidewire and tools during a TriClip procedure which is performed to repair the tricuspid valve by reducing the amount of regurgitation as seen in Doppler ultrasound imaging. The designed system potentially facilitates the positioning of the TriClip at the coaptation gap by pre-mapping the corresponding site of regurgitation in 3D tracking space. A user-friendly Slicer module was developed to automatically segment the vena contracta of the regurgitant jet from Doppler ICE and place it in 3D space.

Summary for Lay Audience

Heart surgeries have evolved from high-risk open-heart surgeries to much safer minimally invasive procedures. Transcatheter interventions often involve repairing a structural heart disease by accessing the heart through veins and arteries. Thin, wire-like tools such as a guidewire are inserted in the body via limbs and are then used to traverse the vessels using live x-ray technology called fluoroscopy. Once the tools reach the heart, they are then positioned at the pathological, target site and deployed to deliver therapy. This positioning of tools is often facilitated using an external ultrasound probe. In this work, we explore the potential of using a novel intracardiac ultrasound probe (ICE) to assist transcatheter procedures in an image-guided system (IGS). We augment a Foresight ICE probe (Conavi Medical Inc.) with an electromagnetic tracking sensor so the probe's position can be always tracked in 3D space. Calibration methods to track the exact location of the ICE image are described as well. The second objective is to demonstrate the feasibility of using a tracked ICE probe in order to generate a vascular roadmap which can then be followed by a tracked guidewire to navigate the vessels. We designed an ultrasound-realistic vessel phantom and reconstructed the vessel in real-time using deep learning methods. The results indicate that ultrasound technology can be used instead of fluoroscopy to visualize and traverse the vessels. The third objective is to develop an IGS to assist the positioning of a therapeutic device during tricuspid valve repair surgery. Current imaging standards produce suboptimal imaging of the tricuspid valve and it can be challenging to identify the site of tricuspid valve regurgitation. We designed an algorithm to automatically detect the location of the regurgitation site from the color Doppler imaging on a tracked ICE probe. This method helps pre-map the location the clinicians have to target with the therapeutic device. This work demonstrates some of the ways an ICE ultrasound technology can improve and assist the existing procedural workflows by providing more information to the clinicians safely and accurately.

Keywords: Intracardiac echocardiography (ICE), Image-guided system (IGS), Transcatheter interventions, Tricuspid valve repair, Vessel reconstruction, Fluoro-free navigation.

Co-Authorship Statement

This thesis integrates several publications that are published or in preparation for submission. Details regarding the author's contributions to these manuscripts are provided below.

Chapter 2

Reference: Hareem Nisar, John Moore, Natasha Alves, Germain Hwang, Terry M. Peters, Elvis C. S. Chen. "Ultrasound calibration for unique 2.5D conical images", Proc. SPIE 10951, Medical Imaging 2019: Image-Guided Procedures, Robotic Interventions, and Modeling, 1095126 (8 March 2019).

Contributions: This chapter contains work beyond the above-mentioned publication. It also includes an extensive report on the characterization of the Foresight™ ICE probe. My contributions towards the report include experimental setup and design, data acquisition, data analysis and writing of the report. Elvis C.S. Chen assisted with the study design. Terry Peters and Brian Courtney reviewed and edited the report. For the manuscript, my contributions include study design, performing experiments, data collection and manuscript preparation. Natasha Alves and Germain Hwang provided their expertise on the probe design during all stages. Elvis C.S. Chen extended his technical expertise during the calibration process. All authors helped in reviewing and editing the manuscript.

Chapter 3

Reference: Hareem Nisar, John Moore, Roberta Piazza, Efthymios Maneas, Elvis C. S. Chen, and Terry M. Peters. "A simple, realistic walled phantom for intravascular and intracardiac applications", Int J CARS 15, 1513–1523 (2020).

Contributions: My contributions to this study include phantom design, preparation of raw materials, imaging data collection, image analysis, and manuscript preparation. John Moore assisted with phantom making and CAD designs. Roberta Piazza helped with the preparation of materials for the phantoms. Efthymios Maneas extended his expertise in phantom making and editing the manuscript. All authors helped in reviewing and editing the manuscript.

Chapter 4

References: Hareem Nisar, Leah Groves, Leandro Cardarelli-Leite, Terry M. Peters, and Elvis C.S. Chen. "Toward Fluoro-Free Interventions: Using Radial Intracardiac Ultrasound for Vascular Navigation", Ultrasound in Medicine and Biology (UMB), (2022)

Hareem Nisar, Patrick K. Carnahan, Djalal Fakim, Humayon Akhuanzada, David Hocking, Terry M. Peters, and Elvis C. S. Chen. "Towards ultrasound-based navigation: deep learning based IVC lumen segmentation from intracardiac echocardiography," Proc. SPIE 12034, Med-

ical Imaging 2022: Image-Guided Procedures, Robotic Interventions, and Modeling, 1203422 (4 April 2022)

Contributions: My contributions include the study design, software development, data collection and analysis, and manuscript writing. Leah Groves assisted with the ultrasound reconstruction pipeline and manuscript editing. Leandro Cardarelli-Leite provided his expertise in designing the study and structuring the manuscript. Patrick Carnahan assisted during the software development stage involving deep learning. Djalal Fakim and Humayon Akhuanzada established the ground truth segmentation. David Hocking supervised the process of defining ground truth and made corrections. All authors helped in reviewing and editing the manuscript.

Chapter 5

Reference: Hareem Nisar, Djalal Fakim, Daniel Bainbridge, Elvis C. S. Chen, and Terry Peters. “3D localization of vena contracta using Doppler ICE imaging in tricuspid valve interventions”, Int J CARS (2022).

Contributions: My contributions to this work includes study design, data collection, development of the methods, data analysis, and writing. Djalal Fakim was responsible for the manufacturing of the patient-specific valve models and imaging the beating heart phantom for data acquisition. He also contributed towards the writing of the final manuscript. Daniel Bainbridge provided clinical expertise in designing the research question and establishing the clinical need. All authors helped in reviewing and editing the manuscript.

Acknowledgements

Although as Ph.D. students, we are encouraged to take ownership of our work, I believe it to be a collaborative (ad)venture. This thesis would not be the same if it weren't for the support of many wonderful individuals – and a cat.

I would like to thank my supervisor, Dr. Terry Peters, for providing me with this opportunity to conduct research and for having faith in my abilities all the way through. From my first interview in a small town in Pakistan to presenting my work internationally in Japan and everything in between (read: 5 years of PhD and a pandemic), Terry has been a constant source of encouragement, guidance, and support. He leads with both brilliance and kindness and has inspired me to be a similar scientist. Thank you for being a mentor to me.

I would also like to thank Dr. Elvis Chen and John Moore for their patience and energy spent in explaining the concepts to me, helping me design studies, as well as giving me the courage to take on challenges. I learned to overcome my fear because John encouraged me to experiment with the new ICE technology and “break a probe”. A great deal of gratitude goes toward the members of my advisory committee – Dr. James Lacefield and Dr. Dan Bainbridge, as well as clinicians – Dr. Hocking and Dr. Leite for their valuable discussions and feedback throughout my degree. Their suggestions have indeed steered this research to be clinically relevant. This work would not have been possible without the research collaboration and support of Conavi Medical Inc. with special thanks to Bogdan Neagu, Feng Patrick Li, and Brian Courtney.

To the members of the VASST lab – thank you for creating a welcoming environment for me and being open to helping solve many, many problems I encountered over the years. A special thanks to Wen Yao, Uditha, and Joeana for listening to my rants, and Leah and Patrick for always debugging my code with me. Dan, Djalal, Michellie, Shuwei, and my two Italian geniuses – your presence made the lab a fun place to work in. Thank you to the “Lab Moms” for being there for all of us.

To my friends – Sarah & El, Jo & Jo, and Gavin who gave me a family away from home and took care of me like their own. I owe my sanity to your support and delicious cooking. Gavin, I don't have the words to describe the amount of faith and encouragement you gave me. Thank you. Last but not least – a ton of gratitude towards my family who supported my dream of being an academic. It was not easy living so far away from you, but your love and prayers kept me going. Thank you Ammi and Abbu for giving me the best possible life – full of love, ease, comfort, science, education, respect, and kindness. My peers, friends, and family – you have always lifted me and talked me into embracing my strengths. I would not have achieved this without your care. I thank God for bringing me to this point in my life and for blessing me with such an amazing support system.

Contents

Abstract	ii
Summary for Lay Audience	iii
Co-Authorship Statement	iv
Acknowledgements	vi
List of Figures	xii
List of Tables	xviii
List of Appendices	xix
1 Introduction: Ultrasound Guidance in Transcatheter Cardiac Interventions	1
1.1 Cardiology	1
1.1.1 Cardiac Anatomy	1
1.2 (R)evolution of Cardiac Therapy	3
1.2.1 Open-Heart Surgeries	3
1.2.2 Minimally Invasive Cardiac Surgeries	4
1.2.3 Micro-invasive Cardiac Surgeries	6
1.3 Transcatheter Cardiac Interventions	6
1.3.1 Introduction	6
1.3.2 Vascular Access	8
1.3.3 Stages	9
Navigation	9
Positioning	10
1.3.4 Interventional Imaging	10
X-ray Fluoroscopy	10
Ultrasound	11
Computed Tomography	13

	Magnetic Resonance Imaging (MRI)	13
1.3.5	Advantages	14
1.3.6	Complications	15
	Fluoroscopy-related complications	16
	TEE-induced complications	17
	Procedural Complications	18
1.3.7	Interventional Challenges	19
1.4	Image Guidance Systems (IGS)	20
1.4.1	Barriers	23
1.4.2	Components	24
	Spatial Tracking	24
	Registration	27
1.5	Interventional Ultrasound	28
1.5.1	Types of Echocardiography	28
1.5.2	Intracardiac Echocardiography	31
1.5.3	Foresight™ ICE	31
1.6	Thesis Outline	31
1.6.1	Chapter 2: Characterization and Calibration of a 2.5D Radial Ultrasound	33
1.6.2	Chapter 3: Towards Vessel Navigation: Ultrasound-realistic, Dual-layered Vessel Phantom	33
1.6.3	Chapter 4: Towards Vessel Navigation: Deep Learning-based ICE-Guidance System to Generate a Vascular Roadmap	34
1.6.4	Chapter 5: Towards Tool Positioning: Localization of Regurgitation Site in Tricuspid Valves using ICE	34
1.6.5	Chapter 6: Conclusion and Future Directions	34
2	Characterization and Calibration of Foresight™ ICE	35
2.1	ICE Image Characterization	36
2.1.1	Image Geometry	37
2.1.2	Image Orientation	38
2.1.3	Image Data Acquisition	39
2.1.4	Image Display Size	41
2.1.5	First Scan-Line Consistency	45
2.1.6	Imaging Angle Accuracy	49
2.1.7	Image Artifacts	50
2.2	ICE Image Visualization	52

2.2.1	Volume Reconstruction and Rendering	52
2.2.2	Surface Texture Mapping	52
2.2.3	DICOM reconstruction and custom interpolation	53
2.3	ICE Probe Calibration	55
2.3.1	Methods	57
2.3.2	Calibration	57
	Spatial Calibration	57
	Temporal Calibration	59
2.3.3	Validation	59
	Calibration Precision	60
	Point Source Localization	60
	Spherical Phantom Centroid	61
2.3.4	Results	62
2.3.5	Calibration	62
	Spatial Calibration	62
	Temporal Calibration	62
2.3.6	Validation	62
	Calibration Precision	63
	Point Source Localization	64
	Spherical Phantom Centroid	65
2.3.7	Discussion	65
2.3.8	Conclusion	67
2.4	Characterization of ICE Calibration	67
2.4.1	Repeatability of Spatial Calibration	68
2.4.2	Intra-procedural positioning	69
2.4.3	Calibration Uniformity wrt Imaging angle	71
2.4.4	Tracking accuracy wrt Imaging Angle	73
2.5	Challenges and Conclusion	74
3	Towards Vessel Navigation: Ultrasound-realistic, Dual-layered Vessel Phantom	76
3.1	Introduction	76
3.2	Materials and Methods	79
3.2.1	Mould and container design	80
3.2.2	PVA-c preparation	83
3.2.3	Vessel-mimicking layer	83
3.2.4	Tissue-mimicking layer	84

3.2.5	Ultrasound imaging	84
3.2.6	Computed tomography (CT) imaging	85
3.3	Results	85
3.4	Discussion	86
3.5	Conclusion	92
4	Towards Vessel Navigation: Deep Learning-based ICE-Guidance System to Generate a Vascular Roadmap	93
4.1	Introduction	93
4.2	Materials and Methods	96
4.2.1	Data Acquisition	96
4.2.2	Pre-processing	98
4.2.3	Lumen Segmentation	98
	Training Data Collection	99
	Deep learning based segmentation	99
	Segmentation evaluation	101
4.2.4	Vessel Reconstruction	101
4.2.5	Validation	102
4.3	Results	102
4.3.1	Vessel Lumen Segmentation	102
4.3.2	Vessel Reconstruction	102
4.4	Discussion	104
4.5	Conclusion	106
5	Towards Tool Positioning: Localization of Regurgitation Site in Tricuspid Valves using ICE	107
5.1	Introduction	107
5.2	Materials and Methods	111
5.2.1	Materials	111
5.2.2	TV modeling procedure	111
5.2.3	Data Collection	112
5.2.4	Data Processing	113
5.2.5	Validation	115
5.3	Results	115
5.4	Discussion	116
5.5	Conclusion	118

6	Conclusions	120
6.1	Thesis Contributions	120
6.2	The New ICE Age	123
6.3	Future Directions	126
	Bibliography	128
A	Codes for ICE Visualization	152
A.1	Code for Conical Volume Reconstruction From a 2D Image	152
A.2	Code for Texture Mapping an Image to a Cone Model	154
A.3	Code for Volume Reconstruction from a DICOM file	156
B	Permissions and Copyrights	161
	Curriculum Vitae	172

List of Figures

1.1	Illustration of the cross-sectional view of the heart with common anatomical features [157]	3
1.2	Comparison of features between the conventional open-heart surgery (left), minimally invasive cardiac surgeries (middle), and micro-invasive or transcatheter interventions (right)	5
1.3	[166] – Overview of common transcatheter valve repair therapies	7
1.4	Common vascular access sites used during percutaneous, transcatheter interventions	8
1.5	[82] Image guidance during a tricuspid valve repair intervention using Cardioband where fluoroscopy (left) is used to align the device (pointed by the arrow) perpendicular to the right coronary artery (RCA), followed by the positioning of the device in the right atrium (RA) under intracardiac ultrasound imaging.	12
1.6	[82] (left) Pre-procedural assessment of the tricuspid valve anatomy using CT volume by measuring the TV annulus diameters. (right) Assessment of right ventricular volume and remodeling using cardiovascular MRI.	14
1.7	List of complications induced due to the use of a TEE probe in an intervention .	17
1.8	(left) A case of device embolization as seen in a projected fluoroscopic image where the arrow points to a misplaced device inside the body, and (right) a case of tamponade resulting in pericardial effusion [127].	19
1.9	Proposed framework by Dilley et al. [64] for the evaluation of an image guidance system	23
1.10	Major components of an image guidance system (IGS)	25
1.11	(left) Aurora tabletop field generator by NDI (Waterloo, ON), and (right) its magnetic field measurement volume [8]	26
1.12	5 DOF and 6 DOF electromagnetic tracking sensors by NDI [3]	27
1.13	Types of echocardiographic probes and their positioning in the human body. . .	30
2.1	Ultrasound image acquisition by the Foresight™ ICE probe as a conical geometry	38

2.2	(a) Side-viewing and (b) forward-viewing modes of Conavi's Foresight™ ICE probe with larger imaging angle and smaller imaging angle respectively.	38
2.3	(a)(b) Different views of conical ICE image in side-viewing mode as seen on Hummingbird console. (c) ICE image view, as seen from inside the cone. (d) Default or 'Home' view of the ICE, as seen from the apex of the cone. (e) A forward-looking ICE image at a smaller imaging angle and (f) its default apical view.	39
2.4	Screenshot of Conavi's Hummingbird console, displaying a conical ICE image from the apical view.	40
2.5	Reconstruction of the 2.5D conical surface image from a 2D circular image, given a value for imaging angle phi.	41
2.6	Radius of the circular echo image displayed on the console vs. the imaging angle at which the ICE image is acquired. Each color represents a different imaging depth or FOV for which the imaging angles are swept from minimum to maximum.	42
2.7	Radius of the circular echo image displayed on the console vs. the imaging angle at which the ICE image is acquired for probe B (left) and probe C (right) at 65mm FOV. Data points are subsampled for display purpose only.	43
2.8	Curve fitting to the absolute radius vs imaging angle dataset acquired at 65 mm FOV for probes A, B and C	44
2.9	Curve fitting to the normalized radius vs imaging angle dataset acquired at 65 mm FOV for probes A, B and C. Data points are subsampled for display purpose only.	45
2.10	Action steps for trials 1-5. The camera icon represents where the image was acquired.	47
2.11	(left) Reference image from Trial 1 overlaid by the centroids from all the trials. (right) Looking closely at the spatial distribution of centroids obtained. .	47
2.12	Displacement of each sample point relative to the centroid from the first scan line of the first image of Trial 1 obtained.	48
2.13	ICE imaging in water bath showing (a) central white-out donut artifact and ring artifact, (b) ring artifact overlaying a reflection from a silicone sheet. Ring artifact is minimized by using the 'magic-wand' button a (c) medium and (d) highest setting.	50
2.14	(a) Sprinkler artifact seen as a foreground. (b) Sprinkler artifact variation (enhanced) seen in the background and (c) brightness adjusted to minimize the background sprinkler effect.	51

2.15	(a) ICE image as seen on the console, (b) after volume reconstruction and rendering in 3D space, and (c) after texture mapping to a cone model via Slicer module.	52
2.16	Schematics of texture mapping of ICE image to a cone model	53
2.17	Schematics of storing radial and spinning ultrasound beams (right) acquired via Foresight™ ICE probe as DICOM file (left)	54
2.18	(a) Conical ultrasound image reconstructed from the DICOM file and with interpolation factor of (b) 5 and (c) 15.	55
2.19	Scanning method for Foresight™ ICE probe - a single element, mechanically rotating transducer acquires data along the radial vector in a spherical coordinate system	56
2.20	(a) Screen capture of Foresight™ ICE image as seen on the Hummingbird console and (b) experimental set up for data acquisition. Arrow shows the reflection of the needle as seen in the ultrasound image.	58
2.21	Validation phantom: (a) cross wire to model a point source, (b) as seen in 2.5D ultrasound and (c) sphere ball, (d) as seen in 2.5D ultrasound.	61
2.22	Normalized signals, derived from the tracker position of the line-object and its reflection in the ultrasound image, before and after temporal calibration is applied.	62
2.23	Qualitative validation of calibration method in virtual space. Needle passing through the reconstructed 2.5D ICE image: (a) side view, and (b) top view. . . .	63
2.24	Outline of experimental steps taken to collect data for the characterization of calibration and tracking behavior of the Foresight™ ICE probe	68
2.25	Error distribution among the three trials	69
2.26	Target registration error (vertical axis) plotted against the radial distance at which it was observed.	70
2.27	(left) Average TRE and (right) standard deviation in TRE heatmaps when the probe is calibrated at a certain angle and validated with imaging at certain angles for Trial 2.	72
2.28	(left) Average TRE and (right) standard deviation in TRE heatmaps when the probe is calibrated at a certain angle and validated with imaging at certain angles for Trial 3.	72
2.29	Distribution of TRE with respect to imaging angle at which the ICE probe is calibrated and validated.	74

2.30	(a) Slicer view of a tracked needle (virtual green line) intersecting its reflection in the ICE image right after calibration is performed, holding the ICE probe static. (b) Error introduced into the tracking environment when the probe is moved.	75
3.1	Conavi Foresight™ ultrasound imaging (ICE) of swine inferior vena cava (IVC) showing variations in the appearance of a vessel. Image (b) and (d) represent the targeted ultrasound imaging aimed in this study. The central dark/bright spot represent the inherent imaging probe artefact.	78
3.2	Overall workflow for fabrication of two layered vascular phantom. Stage 1 involved preparation of vessel-mimicking material (VMM) by mixing polyvinyl alcohol cryogel (PVA-c) with talcum powder as scattering agent and subjecting to freeze-thaw cycles (FTCs). Stage 2 involved preparing and combining tissue-mimicking material (TMM) with solidified VMM. *Fig. 3.5, †Fig. 3.6, ‡Fig. 3.7	79
3.3	CAD model of vessels representing inferior vena cava (IVC) and renal veins. Extended core for support can be seen at the ends.	82
3.4	CAD model of (a) mould to be filled with vessel-mimicking material and core elements; (b) container to create a tissue-mimicking block.	82
3.5	Solid parts of phantom, 3D printed in poly-lactic acid (PLA) plastic material. From left to right: disassembled core elements with collinear cylindrical joints; cope and drag for the mould; bottom and top half of the custom container . . .	83
3.6	(a) Vessel-mimicking material (VMM) after FTCs, still present inside mould. (b) Solidified VMM with core placed inside the custom container, before filling with tissue-mimicking material. The insert in the oblique bifurcation was printed with white PLA, the other inserts with black PLA.	84
3.7	: (a) Tissue-mimicking layer after freeze-thaw cycles, still present inside container. (b) Vascular phantom, with tissue and vessel-mimicking layers, accompanied by an optional silicone padding layer	85
3.8	Conavi Foresight™ intracardiac ultrasound (ICE) imaging of (a) phantom A, (b) phantom B and (c) phantom C, at a radial depth of 5 cm and with time gain compensation (TGC) to suppress the edges of phantom. Phantom A and B show weak reflections from the vessel-mimicking layer, while B depicts increased backscatter from tissue-mimicking material. Phantom C shows strong reflections from the vessel-mimicking layer. Concentric circles in the middle represent inherent imaging probe artefact.	87

3.9	Conavi Foresight™ ultrasound imaging (ICE) of Phantom C (a)(b) at a radial depth of 8 cm showing main vessels and bifurcations, (c) and with time gain compensation (TGC), showing strong reflections from the vessel-mimicking layer and adequate scattering in the tissue-mimicking material. (d) Swine inferior vena cava (IVC) imaged using Foresight™ ICE at a radial depth of 8 cm.	88
3.10	Cross-section of the CT scan of the phantom with average lumen diameter of the main vessel and bifurcations, and infra-renal angle measurements.	89
4.1	Concept diagram for ultrasound-reconstructed vascular roadmap (in blue) used to navigate a tracked guidewire towards the heart.	96
4.2	Data acquisition setup - Ultrasound probe scans the vessel phantom present within the tracking space.	97
4.3	(a) Image data acquired using a frame-grabber as a 2D projection of the conical ultrasound. (b) Lumen segmentation (boundary) achieved using the initial seed (solid). (c) Conical reconstruction of the ultrasound image and the lumen segmentation.	98
4.4	Overall workflow for methods - Intracardiac ultrasound (ICE) imaging dataset is pre-processed and used to train a U-net model via the MONAI framework. Data augmentation is applied during network training. The segmentation labels generated by the U-net are processed to produce the final segmentation output.	100
4.5	Image a) depicts the skeleton of the vessel comprised of spatially calibrated segmentations, Image b) depicts the ultrasound (US) reconstruction registered to the segmented CT scan of the phantom, and Image c) provides a visualization of the surface-to-surface distance analysis between the US and CT models.	103
4.6	Performance of our trained U-net model in the presence of an artifact due to a stent (top) and a lead (bottom) in the vessel.	106
5.1	Three patient specific tricuspid valves modeled using silicone and darcon strings.	112
5.2	Experimental setup - Ultrasound images are acquired using a frame grabber from the Conavi's Hummingbird console. A tracked ICE probe is positioned inside a beating heart phantom to image the patient-specific tricuspid valve. Image and tracking information is sent to a 3D Slicer module for processing.	113
5.3	(a) Sequence of Doppler ICE imaging with maximum regurgitant flow. (b) Imaging sequence containing Doppler information only undergoes maximum intensity projection to create (c) a resultant image with all the highest-velocity Doppler information. This resultant image is then converted to (d) a grayscale image for further processing.	114

5.4	(a) Resultant Doppler image overlayed with the segmentation of the regurgitant jet. (b) Principal component analysis of the segmented region to derive the location of the vena contracta (VC). VC localization seen on (c) a 2D image and in (d) 3D tracking space.	114
5.5	Error bars representing the minimum distance between the algorithm-detected vena contracta location and the ground truth model. For each of the valves, one high error bar can be seen as an outlier.	116
5.6	A qualitative analysis of the results showing the ICE-derived vena contracta locations as points and the ground truth vena contracta as a model (in yellow). A pre-mapped annulus model and vena contracta location in a tracked environment can provide more contextual landmarks for device positioning	117
6.1	Advantages and disadvantages of intracardiac ultrasound (ICE) imaging	123

List of Tables

1.1	Objectives of an Image guidance system (IGS) and their impact	22
1.2	Characteristics of Aurora v2– an electromagnetic tabletop field generator	26
1.3	Comparison of common intracardiac echocardiography (ICE) probes commercially available in 2017.	32
2.1	Precision of spatial calibrations performed at different imaging angles. The overall mean, root mean square (rms) error and 95% confidence interval is given for estimated spatial calibration parameters: translations (t_x, t_y, t_z), Euler rotations (r_x, r_y, r_z) and scaling factors (s_x, s_y, s_z)	63
2.2	Precision of temporal calibrations performed multiple times at different imaging angles	64
2.3	Accuracy of calibrated and tracked Foresight TM ICE probe described in terms of mean standard error and 95% confidence limits for point source localization and sphere location estimation.	65
3.1	Overview of the three phantom versions and their variable parameters – scattering agent concentration in VMM and TMM, and number of FTCs vessel-mimicking layer is subjected to before adding TMM	80
3.2	Recommended values for talcum powder concentration in 10 % w/w polyvinyl alcohol cryogel (PVA-c) to form vessel-mimicking material (VMM) and tissue-mimicking material (TMM), and the number of freeze-thaw cycles (FTCs), the VMM should be subjected to before adding TMM.	89
4.1	Quantitative evaluation of segmentation pipeline using the DICE coefficient of output labels corresponding to the testing dataset.	103
4.2	Summary of the metrics use to quantify the spatial overlap and boundary accuracy of the ultrasound reconstructed vessel compared to the vessel segmented from the CT scan of the phantom.	104
6.1	Comparison of 4D intracardiac echocardiography (ICE) probes commercially available in 2022.	125

List of Appendices

Appendix A: Codes for ICE Visualization	152
Appendix B: Permissions and Copyrights	161

PREVIEW

List of Abbreviations

2D	Two dimensional
2.5D	Two and a half dimensional
3D	Three dimensional
4D	Four dimensional
CT	Computed tomography
ECG	Electrocardiogram
EM	Electromagnetic
FOV	Field of view
ICE	Intracardiac echocardiography
IGI	Image guided intervention
IGS	Image guidance system
IVC	Inferior vena cava
IVUS	Intravascular ultrasound
MRI	Magnetic resonance imaging
MTS	Magnetic tracking system
MV	Mitral valve
PVA-c	Polyvinyl alcohol cryogel
ROI	Region of interest
SVC	Superior vena cava
TAVR	Transcatheter aortic valve repair
TEE	Transesophageal echocardiography

TMM	Tissue-mimicking material
TR	Tricuspid valve regurgitation
TTE	Transthoracic echocardiography
TV	Tricuspid valve
US	Ultrasound
VMM	Vessel-mimicking material

PREVIEW

Chapter 1

Introduction: Ultrasound Guidance in Transcatheter Cardiac Interventions

Transcatheter cardiac interventions face the challenges of invisible tool phenomena, not having a line-of-sight with the anatomy, and relying on 2D fluoroscopic imaging, which is known to cause harmful radiation exposure and spinal issues in the interventional team due to the need to wear heavy lead-lined aprons. In this thesis, we address these challenges by designing image guidance systems (IGS) to facilitate the different stages of a transcatheter cardiac procedure using electromagnetic (EM) tracking technology and intracardiac echocardiography (ICE). We first characterize, calibrate, and track a novel ForesightTM ICE probe so it may be used in an IGS. Then, an ICE-generated vessel reconstruction method is developed to facilitate fluoro-free tool navigation. Finally, the tracked ICE probe is used in a Doppler mode to identify the site of tricuspid valve regurgitation in 3D space and facilitate the device positioning step during valve repair interventions. This chapter provides the necessary background information and overview of the state-of-the-art technology relevant to the work performed in this thesis.

1.1 Cardiology

1.1.1 Cardiac Anatomy

The heart is the *heart* of the human body as it supplies and regulates blood flow throughout the circulatory system to keep the rest of the body alive. This complex and dynamic organ continuously beats by means of muscular contractions to maintain the blood flow. It is positioned slightly left to the mediastinum in the chest, and in humans, there are four cardiac chambers – two atria and two ventricles, along with two atrioventricular valves namely the tricuspid valve (TV) and the mitral valve (MV). The right atrium, the tricuspid valve, and the right ventricle

are collectively referred to as the ‘right-sided heart’. Similarly, the left atrium, the mitral valve, and the left ventricle are called the ‘left-sided heart’. The left and right atria are separated by a thin wall of tissue called the atrial septum, that needs to be punctured when a left-sided transcatheter procedure is performed. From a therapy perspective, there are many differences in the left and right sides of the heart including the anatomy of the atrioventricular valve, the pressures on each side, and the means of access to the desired anatomical structure.

The pressure on the left side of the heart is around three times higher than that on the right side, and by approximately 8mmHg on average and is mainly due to the function each side is performing. The muscles on the left side are stronger as well since they have to pump the oxygenated blood to the entire body including the extremities. On the other hand, the right-sided heart supplies blood to the lungs with fewer vessels and less resistance, thus requiring lower blood pressure and pumped by less powerful heart muscles. For this reason, there is a high risk of perforation during right-sided heart surgery or therapy.

The nature of mitral and tricuspid valve surgeries/therapies differ significantly as these valves differ greatly in their anatomy and positioning. The mitral valve has two leaflets that are connected to the papillary muscles using tendinous chords (chordae tendinae) or “heart strings”. Due to its posterior location, close to the esophagus, the MV can be visualized well using standard cardiac ultrasound or transesophageal echocardiography (TEE) views. As such, mitral valve therapies have been well developed and standard protocols exist in clinical practice. Meanwhile, tricuspid valve therapies and imaging protocols are currently underway. As the name suggests, the tricuspid valve has three leaflets that regulate the blood flow between the atrium and the ventricle. It is positioned such that the TEE probe is parallel to the TV annulus and at a significant distance, thus causing signal dropout in the ultrasound (US) imaging. Moreover, the chordae are more complicated in the case of the TV, with the chordae tendinea attaching the leaflets to the papillary muscles as well as directly to the walls of the right ventricle.

This thesis deals primarily with transcatheter interventions which are often performed to repair structural heart diseases. During these interventions, the heart is accessed using either the inferior vena cava (IVC) or the superior vena cava (SVC) which opens directly into the right atrium. The tricuspid valve can be accessed by entering in the right atrium and bending the catheter at roughly 90 degrees. To access the left atrium or the mitral valve, the catheter first needs to enter the right atrium and then puncture the atrial septum to be advanced into the left atrium. Transseptal puncture is a meticulous procedure with an associated risk of aortic valve puncture or pericardial perforation.

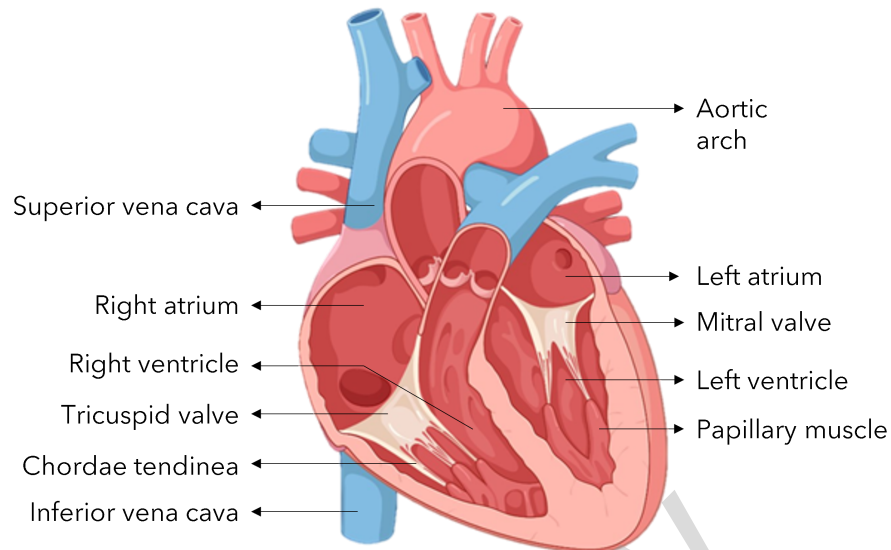


Figure 1.1: Illustration of the cross-sectional view of the heart with common anatomical features [157]

1.2 (R)evolution of Cardiac Therapy

This thesis strongly advocates for percutaneous, transcatheter, cardiovascular interventions as opposed to open-heart surgeries. We, as humankind, have come a long way towards simplifying the surgical procedures for the heart and are still progressing. From the first successful heart surgery by Dr. Ludwig Rehn in 1896 to repair a stab wound, to the revolutionary invention of the cardiopulmonary by-pass machine and the development of Cath labs and interventional suites – surgery has continuously improved with technological advances [39, 69]. Today, well-established techniques in cardiac surgery can further benefit from modern technology to enhance patient safety, minimize the concerns of the medical staff, and reduce the time for hospitalization. This section looks at the different categories of cardiac surgery and therapy i.e., the evolution of open-heart surgery, to minimally invasive cardiac surgeries and transcatheter procedures. A comparison of these major surgical categories can be seen in figure 2.

1.2.1 Open-Heart Surgeries

Cardiac surgery was clinically initiated in the early 1940s when only a few procedures, including the closure of a patent ductus to separate the two merged blood vessels, repair of aortic coarctation or narrowing, the Blalock-Taussig shunt to increase the blood flow to the lungs, and the mitral commissurotomy to repair mitral valve stenosis could be performed [189]. Atrial septal defect closure was tried using techniques such as hypothermia and the Gross well [58],